Hindawi
Advances in Materials Science and Engineering
Volume 2022, Article ID 8196347, 12 pages
https://doi.org/10.1155/2022/8196347

Research Article

Analysis of Turning Performance on AISI O1 Steel Using VO+nMoS$_2$ as Coolant

V. Sivaraman,[1] S. J. Davis Hans,[2] Kumaran Palani,[3] Tsegaye Alemayehu Atiso,[4] Jafferson JM,[5] and Nimel Sworna Ross[6]

[1]*Department of Mechanical Engineering, Panimalar Polytechnic College, Chennai, India*
[2]*Department of Mechanical Engineering, Jansons Institute of Technology, Coimbatore, India*
[3]*Department of Mechanical Engineering, College of Engineering, Wolaita Sodo University, Wolaita Sodo, Ethiopia*
[4]*Dean for College of Engineering, Wolaita Sodo University, Wolaita Sodo, Ethiopia*
[5]*Director CoE for Additive Manufacturing, VIT University, Chennai Campus, Vellore, India*
[6]*Department of Mechanical Engineering, Saveetha School of Engineering, Saveetha Institute of Medical and Technical Sciences, Chennai 602105, Tamil Nadu, India*

Correspondence should be addressed to Kumaran Palani; pkumaran2003et@gmail.com and Nimel Sworna Ross; nimelross@gmail.com

Received 14 February 2022; Revised 15 March 2022; Accepted 28 March 2022; Published 23 April 2022

Academic Editor: Adam Khan M

AISI O1 cold work steel is a hard-to-machine material as a reason of its good temperature resistance, superficial hardness, and lesser response to wear. Hence, material removal from such hard materials is both cost- and time-consuming. Conventional cutting fluids fail to lessen the hotness at the tool-work junction. This research work explores the effects of a uniquely prepared and eco-friendly cutting fluid on the cutting performance of AISI O1 steel using tool inserts of three different materials. The prepared cutting fluid, molybdenum disulfide nanoparticle (MoS2) blended in biodegradable vegetable oil (VO) was distributed into the cutting zone with the help of the minimum quantity lubricant (MQL) technique. The integrated approach of Taguchi's average normalized S/N ratio-based RSM method was employed to model the parameters for better responses. The optimal condition predicted by the approach (the type of insert – CBN, Vc – 110.12 m/min, f – 0.08 mm/rev, and DOC – 0.20076 mm) was observed to produce noteworthy improvements in tool wear and lessen the cutting force in addition to a good surface finish. The study will offer the required guidance for tool and die industries handling AISI O1 steel and help researchers work towards sustainable machining.

1. Introduction

AISI O1 is a cold worked, low alloy steel with high demand in industries manufacturing tools and dies [1]. It is an oil-hardening tool steel with higher chromium and tungsten content and hence an improved wear resistance. It has an elevated hardness of 56–62 HRC because of its high carbon content and high resistance to wear at moderate temperatures (Navas et al. 2008). The machining of quenched steels is accomplished by employing grinding wheels due to their increased hardness [2]. High temperatures produced during dry machining diminish the strength of cutting tools because of plastic deformation [3]. An investigational trial on dry machining of 17–4 PH stainless steel has detected more cutter wear due to its higher temperature at the cutting zone [4]. Heavy mechanical and thermal loading during dry cutting results shows severe imperfections on the machined surface, such as grooves creating microfracture and smearing [5]. Hence, the heat evolved in the machining region must be controlled effectively by an appropriate selection of correct machining parameters with effective cutting fluids (CFs) [6]. The CFs are not only used for the lubrication process but also to provide good cooling and clearing of chips from the machining zone. The tribological features of CFs create a thin protective film layer over the machining zone, reducing the friction and wear [7]. Conventional CFs make a stringent environmental impact, affecting employee health. The production cost is increased for

separating the chips from CFs [8]. In the MQL technique, also known as near-dry machining, a minor amount of vegetable-based oil or biodegradable synthetic esters were delivered along with compressed air to the site of machining in the range of 10–100 ml/hr [9]. It was found that the approach has provided significant improvements in machined surfaces and the life of cutting tools [10]. The MQL method minimized the cutter wear and promisingly augmented the material removal rate in the turning of nickel-chromium alloy [11]. MQL improves the cutting tool life and decreases the cutting forces [12]. Response surface methodology (RSM) was explored to investigate the parameter effects in machining titanium alloy under the MQL environment. The developed mathematical equations were observed to predict the performance of turning characteristics close to the investigational results [13]. Experimental investigations quantified that MQL can curtail together manufacturing costs and ecological hazards hence an effective alternative to conventional flood cooling [14]. Biodegradable vegetable oils are used in the MQL technique to induce sustainability during the machining process. Although biodegradable oils have good lubricant qualities, their low thermal properties limit their usage as CFs in the machining industry [15]. Modern-day studies have revealed that distinct nanoparticles are added to the CF to surge the efficacy of the MQL system in the machining method [16]. The polymer polyether ether ketone with varying size and concentration of solid lubricants (MoS2 and WS2) reduced the friction up to 30%. The nano-sized solid lubricant particles reduced the tool wear significantly by providing an effective low friction tribofilm [17]. Greater nanoparticle levels increase the thermal conductivity of nanofluids. MoS2 was found to be nonreactive [18]. The machining characteristics of nano MoS2 in the MQL technique with various base fluids such as palm oil, soyabean oil, rapeseed oil, and paraffin oil were studied. Palm oil effectively decreases the cutting forces and grinding energy, although soya bean oil with a 6% concentration of nMoS2 particles provides more cooling and lubrication than palm oil due to its higher viscosity [19]. The inclusion of nanoparticles in the base CF improves heat conductivity, lowering the cutting temperature [20]. Machining of AISI 1040 steel with nMoS2 with vegetable oil under the MQL technique reduced the coefficient of friction by 37% and cutting temperature by 21% compared to dry machining [21]. RSM is perceived as an interesting tool by many researchers for various applications. The prediction model for surface roughness was formed using RSM to determine the surface quality in the machining process [22]. RSM is a practical method for modelling any industrial process for sustainable manufacturing.

In this view, it was decided to realize the potential of molybdenum disulfide nanoparticles blended with biodegradable vegetable oil on turning. Nanofluid was prepared under laboratory conditions. Traditional dry turning, flood cooling, and nanofluid expelled using the MQL system were employed, and the results were compared. Machining parameters such as cutting speed (Vc), feed rate (f), and depth of cut (DOC) were considered independent variables, and the effect of these parameters on surface roughness, tool wear, and chip morphology has been investigated. In this study, an integrated approach of principal component-based RSM was used for designing, analyzing, and optimizing the hard turning of AISI O1 cold work tool steel.

2. Experimental Procedure

2.1. Material and Tool. CNC lathe, Super Jobber 500 has been used to carry out the turning operations on AISI O1 cold work tool steel. The 50 mm long workpiece is a round bar of 30 mm diameter. Three different types of ISO-designated cutting inserts (PVD-TiAlN, ceramic, and CBN) were used. The inserts were mechanically clamped on tool holders (Teknik PCLNR 2525M12). The experimental setup is shown in Figure 1. The chemical composition of the workpiece is as follows: Fe – 95.4%, Mn – 1.35%, C – 0.90%, Si – 0.37%, Cr – 0.56%, W – 0.47%, Ni – 0.29%, V – 0.30%, Cu – 0.22%, P – 0.03%, and S – 0.03%. Table 1 shows the process parameters of the experimental work.

2.2. Machining Environments. The nMQL was made by dissolving 0.2 %wt. of nMoS2 in 100 ml of castor oil with a mechanical stirrer. Castor oil has a viscosity of 0.535 Pa s. At an air pressure of 8 bar, the MQL system (KENCO brand) was programmed to produce 50 ml/h (flow rate). The distance between the nozzle and tool-work interface was 15 mm with the nozzle directed at a spray angle of 30°. Experiments were conducted for the fixed ranges under controllable process parameters.

2.3. Experimentation. The studies are created following Taguchi's design of experiments concept. Preliminary experimental trials are conducted to identify the most influencing parameters and the range of their levels. The f, depth of cut, and Vc are the most important turning factors, and they can be modified at three levels. The L27 orthogonal array (OA) was chosen to accommodate the turning parameters. The experiments were conducted according to the designed OA at random experimental to avoid the extraneous effects of uncontrollable parameters, and two replications were performed at each condition. Surface roughness (Ra), flank wear (Vb), temperature (T), and cutting force (Fc) are considered as the outcomes influencing the machining performance. The output responses are displayed in Table 2.

2.4. Measurement. A dynamometer was used to evaluate the cutting force. Taylor Hobson Surtronic 3+ was used to quantify the machined surface's roughness. A video measuring system was used to assess tool wear (VMS-1020F). An HTC-IR noncontact thermometer with an accuracy level of ±1 was utilized to quantify the temperature during turning. The surface topography, tool damage, and chip formation were examined using a Hitachi scanning electron microscope (SEM).

Figure 1: Experimental setup.

Table 1: Experimental parameters.

Workpiece	AISI O1 steel
Cutting insert	PVD – TiAlN, ceramic, CBN
Insert model – TiAlN, ceramic, CBN	TNMG 160408 TFTNGA160408T01020 TNMG 160408
Axial DOC (mm) conditions, Vc (m/min)	0.2, 0.45, 0.7 nMQL 110, 140, 170
f (mm/rev)	0.02, 0.05, 0.08
Hardness (HRC)	62
Nose radius (mm)	0.8

Table 2: Experimental condition and observed responses.

		Parameters			Responses							
Ex. No.	Type of insert	Vc	*f*	Depth of cut	Surface roughness, Ra (μm)		Flank wear, Vb (mm)		Temperature, *T* (°C)		Cutting force, Fc (*N*)	
1	TiAlN	110	0.02	0.2	0.602	0.602	0.021	0.021	84	85	345	345
2	TiAlN	110	0.05	0.45	0.934	0.918	0.023	0.023	88	88	332	335
3	TiAlN	110	0.08	0.7	1.334	1.346	0.028	0.028	104	103	358	359
4	TiAlN	140	0.02	0.45	0.664	0.693	0.027	0.026	102	102	321	321
5	TiAlN	140	0.05	0.7	0.764	0.784	0.030	0.029	105	105	349	352
6	TiAlN	140	0.08	0.2	0.590	0.602	0.030	0.029	112	111	359	360
7	TiAlN	170	0.02	0.7	0.570	0.579	0.027	0.027	115	115	285	284
8	TiAlN	170	0.05	0.2	0.544	0.544	0.030	0.031	121	122	337	338
9	TiAlN	170	0.08	0.45	0.824	0.804	0.034	0.034	125	125	378	378
10	Ceramic	110	0.02	0.2	0.620	0.649	0.022	0.022	88	88	315	317
11	Ceramic	110	0.05	0.45	0.790	0.794	0.025	0.025	100	100	326	326
12	Ceramic	110	0.08	0.7	0.970	0.954	0.032	0.033	109	109	348	346
13	Ceramic	140	0.02	0.45	0.770	0.790	0.024	0.023	95	94	325	327
14	Ceramic	140	0.05	0.7	0.870	0.874	0.028	0.028	107	107	392	390
15	Ceramic	140	0.08	0.2	0.740	0.764	0.022	0.021	98	97	253	255
16	Ceramic	170	0.02	0.7	0.480	0.484	0.025	0.025	103	103	276	277
17	Ceramic	170	0.05	0.2	0.450	0.434	0.029	0.028	105	104	321	322
18	Ceramic	170	0.08	0.45	0.670	0.650	0.032	0.032	108	108	342	341
19	CBN	110	0.02	0.2	0.495	0.491	0.022	0.022	83	82	355	354
20	CBN	110	0.05	0.45	0.565	0.549	0.023	0.022	74	74	277	276
21	CBN	110	0.08	0.7	0.635	0.635	0.026	0.025	92	91	354	354
22	CBN	140	0.02	0.45	0.425	0.405	0.023	0.023	96	96	273	274
23	CBN	140	0.05	0.7	0.605	0.625	0.025	0.025	85	85	296	296
24	CBN	140	0.08	0.2	0.535	0.543	0.023	0.022	90	91	268	271
25	CBN	170	0.02	0.7	0.410	0.439	0.024	0.024	103	103	246	247
26	CBN	170	0.05	0.2	0.320	0.349	0.021	0.022	98	98	263	263
27	CBN	170	0.08	0.45	0.425	0.441	0.025	0.025	100	101	289	287

3. Average Normalized S/N Ratio-Based RSM (ASN-RSM)

RSM is a statistical tool with a module on the modelling of variables and optimization of multiple outcomes using the desirability approach. RSM can illustrate the effect of turning parameters via the response surface graphs [22]. When multiples responses are involved in a problem, the RSM technique generates individual polynomial models for each response. For simultaneous optimization, the multiple responses are converted into a single quality index, which is incorporated into necessary algorithms for predicting the optimal condition. The single quality index is fed into the RSM technique to predict the optimal condition of turning parameters. The algorithm of an ASN-RSM is as follows:

Step 1: Estimate the value of the S/N ratio (η_{ij}) for each response using a suitable formula based on its quality characteristics. The S/N ratio condenses the observation with replications of a certain trial by considering the mean and standard deviation of its replications. The observed responses such as flank wear (Vb), temperature (T), and cutting force (Fc) are the "smaller-the-better" quality characteristics.

The goal point of smaller-the-better quality characteristics is the attainment of value 0 (zero). The S/N ratio (η_{ij}) for such a characteristic is evaluated by means of the following equation:

$$\frac{S}{N}\text{Ratio}\left(\eta_{ij}\right) = -10.\ \log_{10}\frac{1}{r}\sum_{i=1}^{r} y_{ij}^{2}, \tag{1}$$

where r is the quantity of repetitions; $i = 1, 2, 3, \ldots, n$; $j = 1, 2, 3, \ldots, m$; m is the number of responses, and n is the number of experimental trials.

Step 2: Compute the normalized S/N ratio (Z_{ij}) using equation (2) to minimize the influence of the variability of the S/N ratio among responses. The values of the normalized S/N ratio vary between 0 and 1.

$$Z_{ij} = \frac{\eta_{ij} - \min\left(\eta_{ij}, i = 1, 2, 3 \ldots, n\right)}{\max\left(\eta_{ij}, i = 1, 2, 3 \ldots, n\right) - \min\left(\eta_{ij}, i = 1, 2, 3 \ldots, n\right)}. \tag{2}$$

Step 3: Analyze the average normalized S/N ratio (ASN) value of each trial using the following equation:

$$ASN_i = \frac{\sum_{j=1}^{m}\left(Z_{ij}\right)}{m}. \tag{3}$$

Step 4: Develop a polynomial regression model that constructs a relationship between ASN and turning parameters to depict the behavior of parameters in the experimental domain.

Step 5: Perform the analysis of variance (ANOVA) with ASN values to find the contribution and statistical significance of different turning parameters on the responses.

Step 6: Make the 3D response surface plots to reveal the effects of parameter levels on the ASN and find out the near-optimal condition of turning parameters using the desirability approach.

Step 7: Conduct the confirmation experiments for authenticating the optimal parameter setting predicted using RSM.

4. Results and Discussion

4.1. Implementation of ASN-RSM. As an initial step of the proposed algorithm, the observed data is transformed as the S/N ratio where the quality characteristics of responses were converted into larger-the-better irrespective of the quality characteristics of responses. The responses are transformed as S/N ratio values of the smaller-the-better condition, and the variability among the S/N ratio of responses is reduced by the normalizing process. The calculated S/N ratio and normalized S/N ratio (NSNR) are shown in Table 3. An individual set of normalized S/N ratio values is obtained for each response procedure, and the normalized S/N ratio values are combined by calculating the average of them. For ensuring the equal importance of responses, the average normalized S/N ratio value is considered for further analysis [23]. The calculated single quality index "average normalized S/N ratio" (ASN) for each trial is presented in Table 3.

The ASN value of experiment number 26 appears high among the set of ASN values, which indicates that the corresponding turning condition is adjacent to the optimal turning condition. The dispersion of ASN values for various trials is plotted and shown in Figure 2. The variation of ASN to the adjacent trial shows that there is minimal effect of extraneous factors on the responses.

4.2. Development of Polynomial Model Using RSM. A second-order polynomial equation was generated using the software Design Expert V7.0 that constructs a relationship between the parameters of the turning process and ASN. The model was reduced by the backward elimination method in which the elimination of insignificant model terms originates from its highest order. The mathematical models to predict the ASN value using coded factors and models for each level of categorical factor "type of insert" are presented in equations (4)–(7), respectively. The pooled ANOVA was established with significant model terms, and the model coefficient is shown in Table 4. The model fitness and model terms are verified at the confident level of 99% and 95%, respectively. The calculated F-ratio of the developed model was 25.06, and p-value was less than 0.0001, displaying model fitness and adequacy of model terms. The model terms A, B, C, D, BC, BD, and CD were identified as significant model terms.

Table 3: Calculated S/N ratio, normalized S/N ratio, and ASN values.

Ex. No.	S/N ratio				Normalized S/N ratio (NSN)				ASN
	Ra	Vb	*T*	Fc	Ra	Vb	*T*	Fc	
1	4.408	33.432	−38.486	−50.756	0.557	1.000	0.758	0.274	0.647
2	0.593	32.956	−38.890	−50.423	0.250	0.884	0.669	0.357	0.540
3	−2.503	30.964	−40.341	−51.078	0.000	0.400	0.351	0.195	0.236
4	3.557	31.437	−40.172	−50.130	0.489	0.515	0.388	0.429	0.455
5	2.338	30.516	−40.424	−50.857	0.390	0.291	0.333	0.249	0.316
6	4.583	30.400	−40.984	−51.102	0.571	0.263	0.209	0.189	0.308
7	4.876	31.437	−41.214	−49.097	0.595	0.515	0.159	0.684	0.488
8	5.288	30.574	−41.656	−50.553	0.628	0.305	0.062	0.324	0.330
9	1.681	29.319	−41.938	−51.550	0.337	0.000	0.000	0.078	0.104
10	4.152	33.311	−38.890	−49.966	0.537	0.970	0.669	0.469	0.662
11	2.047	32.217	−40.000	−50.264	0.367	0.704	0.426	0.396	0.473
12	0.265	29.843	−40.749	−50.832	0.223	0.127	0.261	0.256	0.217
13	2.270	32.432	−39.554	−50.238	0.385	0.757	0.523	0.402	0.517
14	1.210	31.213	−40.588	−51.866	0.299	0.460	0.297	0.000	0.264
15	2.615	33.351	−39.825	−48.062	0.413	0.980	0.464	0.940	0.699
16	6.375	32.217	−40.257	−48.818	0.716	0.704	0.369	0.753	0.636
17	6.936	30.873	−40.424	−50.130	0.761	0.378	0.333	0.429	0.475
18	3.479	29.924	−40.668	−50.681	0.482	0.147	0.279	0.293	0.300
19	6.108	33.073	−38.382	−51.005	0.694	0.913	0.781	0.213	0.650
20	4.959	32.841	−37.385	−48.850	0.602	0.856	1.000	0.745	0.801
21	3.945	31.869	−39.276	−50.980	0.520	0.620	0.585	0.219	0.493
22	7.432	32.803	−39.645	−48.723	0.801	0.847	0.504	0.776	0.732
23	4.365	32.217	−38.588	−49.426	0.554	0.704	0.736	0.603	0.654
24	5.433	32.728	−39.085	−48.563	0.640	0.829	0.627	0.816	0.728
25	7.744	32.324	−40.257	−47.819	0.826	0.730	0.369	1.000	0.745
26	9.897	33.432	−39.825	−48.399	1.000	1.000	0.464	0.857	0.830
27	7.432	31.938	−40.000	−49.218	0.801	0.637	0.426	0.654	0.636

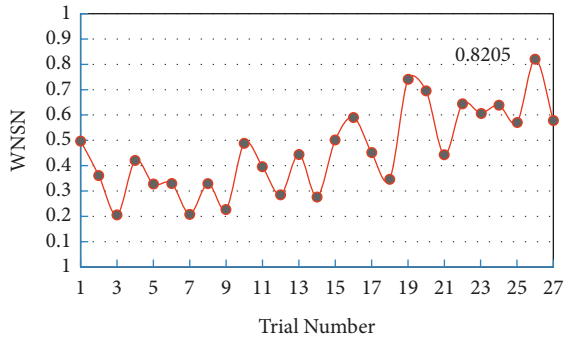

Figure 2: Variation of ASN for different trials.

Table 4: Results of ANOVA on ASN.

Source	Sum of squares	Degrees of freedom	Mean sum of square	*F*-value	*p*-value	Remarks
Model	0.92	10	0.092	13.2	<0.0001	Significant
A – type of coating	0.48	2	0.24	34.02	<0.0001	
B – Vc	0.043	1	0.043	6.21	0.024	
C – F	0.18	1	0.18	26.03	0.0001	
D – depth of cut	0.091	1	0.091	13.03	0.0024	
AB	0.053	2	0.026	3.76	0.0457	
AC	0.038	2	0.019	2.69	0.0985	
CD	0.082	1	0.082	11.78	0.0034	
Residual	0.11	16	7.00E-03			
Cor total	1.04	26				

4.2.1. Final Equation in terms of Coded Factors

$$\begin{aligned}\text{ASN} = {} & +0.52 - 0.14 * \text{A}[1] - 0.045 * \text{A}[2] - 0.062 * \text{B} - 0.10 * \text{C} - 0.071 * \text{D} - 0.074 * \text{A}[1]\text{B} \\ & + 0.020 * \text{A}[2]\text{B} - 0.056 * \text{A}[1]\text{C} + 9.844\text{E} - 004 * \text{A}[2]\text{C} - 0.10 * \text{CD}.\end{aligned} \tag{4}$$

4.2.2. Final Equation in terms of Actual Factors

Insert – TiAlN

$$\begin{aligned}\text{ASN} = {} & +1.09071 - 4.53446\text{E} - 003 * \text{B} + 1.05560 * \text{C} \\ & + 0.41437 * \text{D} - 13.98142 * \text{C} * \text{D}.\end{aligned} \tag{5}$$

Insert – Ceramic

$$\begin{aligned}\text{ASN} = {} & +0.64936 - 1.41701\text{E} - 003 * \text{B} + 2.97103 * \text{C} \\ & + 0.41437 * \text{D} - 13.98142 * \text{C} * \text{D}.\end{aligned} \tag{6}$$

Insert – CBN

$$\begin{aligned}\text{ASN} = {} & +0.62236 - 2.65526\text{E} - 004 * \text{B} + 4.78802 * \text{C} \\ & + 0.41437 * \text{D} - 13.98142 * \text{C} * \text{D}.\end{aligned} \tag{7}$$

The value of coefficient of determination (R^2) was computed as 0.8919, which is nearer to the value 1 and assures the ability of the model in predicting the ASN precisely. There was a closeness between the adjusted R-squared value (0.8244) and the predicted R-squared value (0.6712) that states that the contribution of insignificant terms in arriving at the model fitness is minimum (Table 5). The adequate precision is 13.858, which is greater than 4 that evidences the adequate model discrimination. Moreover, the values of predicted ASN values using the polynomial model and actual ASN values of corresponding machining condition were compared, and the predicted values of ASN fall very closer to the actual values (Figure 3(a)). Figure 3(b) displays the normal probability plot. It was found that the residuals are spread along the straight line closely indicating that normal distribution exists and no other pattern is followed.

4.3. Effect of Parameters on ASN. The ASN value is the single representative of all the responses (surface roughness (Ra), flank wear (Vb), temperature (T), and cutting force (Fc)) and is to be maximized in order to find the optimal cutting condition. The types of inserts contributed to the ASN values significantly. The variation of ASN with the levels of inserts is plotted by varying the Vc (Figure 4(a)). The ASN value was minimum while using the TiAlN insert (0.2445), whereas it appears maximum while using of the CBN insert (0.6884). From Figure 4(a), there is an interaction between ceramic and CBN while varying the Vc (B). The influence of different tool inserts on ASN was plotted for different f (C). It was found that there is no interaction among the levels of tool inserts and the performance of CBN insert (0.7416) was improved at minimum f (Figure 4(b)). Hence, the information from Figure 4 confirms that the insert – CBN produces better values of responses at different cutting conditions of the remaining parameters.

The predicted values of ASN at the Vc of 140 m/min with TiAlN insert were plotted as a 3D response surface graph (Figure 5(a)) by varying the f (C) and DOC (D). The ASN value (0.5718) was better at a lower level of f and higher DOC at a constant Vc. From Figure 5(a), it was found that there is a significant improvement in ASN, when the f is reduced from 0.08 mm/rev to 0.02 mm/rev at a higher depth of cut. There was no substantial improvement in ASN even when the f is reduced at a lower level of DOC (Figure 5(a)). The performance of the machining process was improved with the decrease of DOC (D) at a constant f. The ASN value is enhanced as 0.6047 at the lower level of f (C) and a higher level of DOC (D) with a ceramic insert (Figure 5(b)). A significant influence on ASN is identified with the variation of f (C) from a higher level to lower level at the maximum DOC as well as with the change of DOC (D) at higher f (C) while using ceramic insert (Figure 5(b)). The ASN value reached a higher value (nearer to 0.8271) for the DOC values from 0.7 mm to 0.2 mm, at a constant f of 0.08 mm/rev using CBN insert (Figure 5(c)). The growth rate of ASN was more extensive at a higher level than of lower-level f (C) when the DOC is reduced.

The value of ASN appeared high at the lower level of DOC and higher-level f, while the Vc is maintained at a constant level (Vc = 140 m/min). It was identified that there is a substantial change in ASN value while varying the DOC at a higher level of f (Figure 5(c)). The improvement of the ASN value describes the growth of all the responses, which was maximized at lower DOC (Figure 5(c)).

4.4. Influence of Machining Parameters on Responses. Improved response values are observed while using the CBN insert for turning using nano coolant (Figure 6(a)). A significant improvement was identified in surface roughness, and it is reduced to Ra = 0.48 μm from the value Ra = 0.76 μm obtained with TiAlN insert. The required cutting force is reduced due to the high hardened nature of the CBN insert, and heat generation is also minimal compared to other inserts. The influence of Vc on surface roughness, flank wear, temperature, and cutting force are illustrated in Figure 6(b). Even the higher Vc increases the rate of production, the generation of heat and cutting force is observed to be high due to high friction stress between tool and workpiece. The temperature of the insert varied from 91.3°C to 108.67°C when the Vc is increased from 110 m/min to 170 m/min. The

Table 5: *R*-squared and adequate precision value of the model.

Std. Dev.	0.0837	*R*-squared	0.8919
Mean	0.5161	Adj *R*-squared	0.8244
CV, %	16.2076	Pred *R*-squared	0.6712
PRESS	0.3406	Adeq precision	13.8582

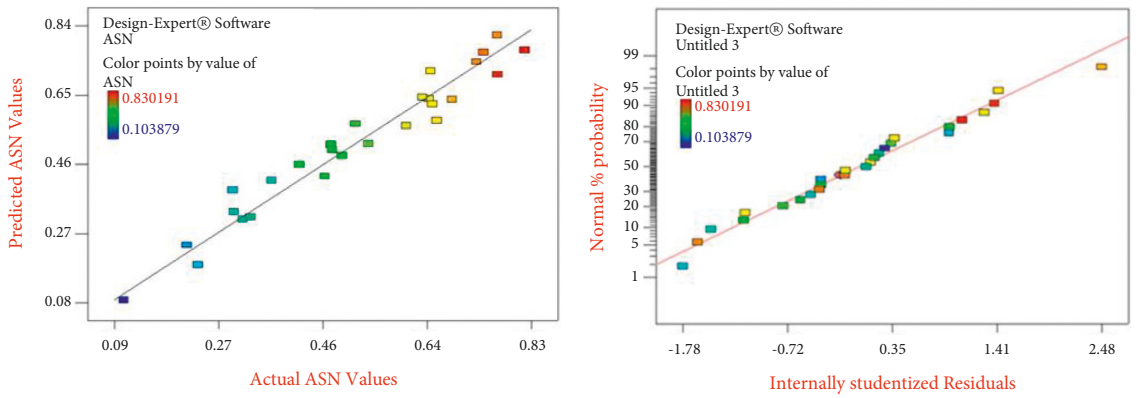

Figure 3: Plot of (a) predicted and actual ASN and (b) normal percentage probability to residuals.

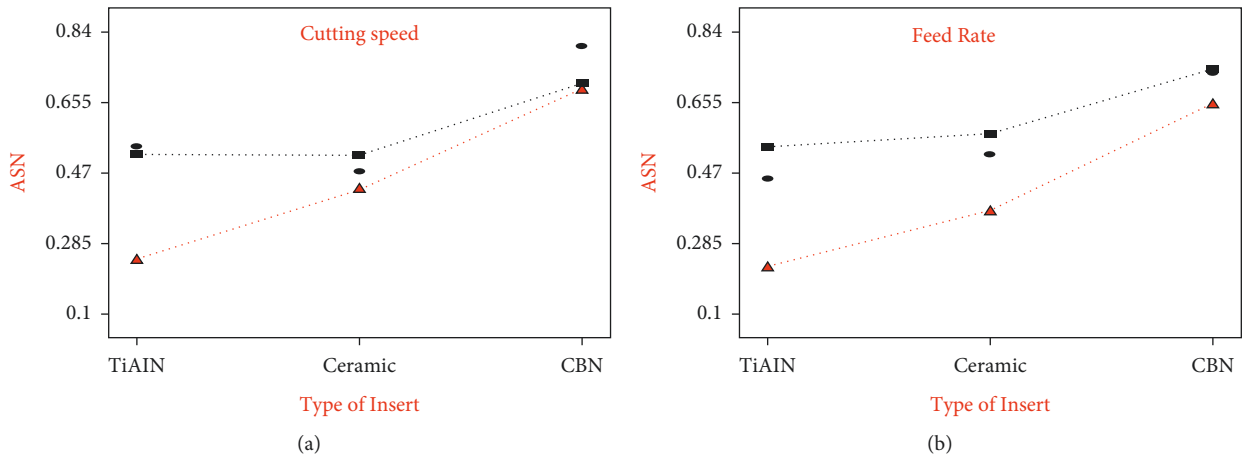

Figure 4: Effect of tool inserts on (a) ASN with cutting speed and (b) ASN with feed rate.

flank wear is enhanced by the thermal softening of the cutting tool due to the high temperature generated at the machining interface. The flank wear is increased at high Vc due to large size of built-up edge (BUE), and the unstable BUE protects the flank face from further wear. An increase in *f* increased the surface roughness (Figure 6(c)). At higher *f*, the gap between peel-off layers was maximum that left ploughing marks and uncut materials on the machined surfaces. Thereby, the surface roughness was measured high, and the required cutting force was also more due to the depth of penetration of the insert along the axis of rotation of the workpiece at a higher *f*. The effect of DOC is shown in Figure 6(d). The higher DOC produces the additional cutting force, which increases the heat generation. At higher temperatures, the responses include poor surface finish and flank wear. Hence, the higher DOC reduces the productivity of the cutting tool.

4.5. Desirability. The parameter setting possessing a higher desirability index is chosen as the optimal setting. The ramp functional graph of the optimal condition is shown in Figure 7. The red dot on each ramp indicates the optimal set of parameters at the most desirable condition. The prediction of ASN appears higher than that of experimental values. Table 6 shows the optimal condition and predicted value of ASN. The predicted optimal condition includes the following: type of insert – CBN, Vc – 110.12 m/min, *f* – 0.079 mm/rev, and DOC – 0.20076 mm. The predicted ASN value at the optimal condition was observed as 0.8328. The expected value falls in the range of 95% confidence interval.

4.6. Validation of Experiments. The confirmation trials were performed with the parameter setting obtained using the ASN-RSM algorithm to validate the efficiency of the

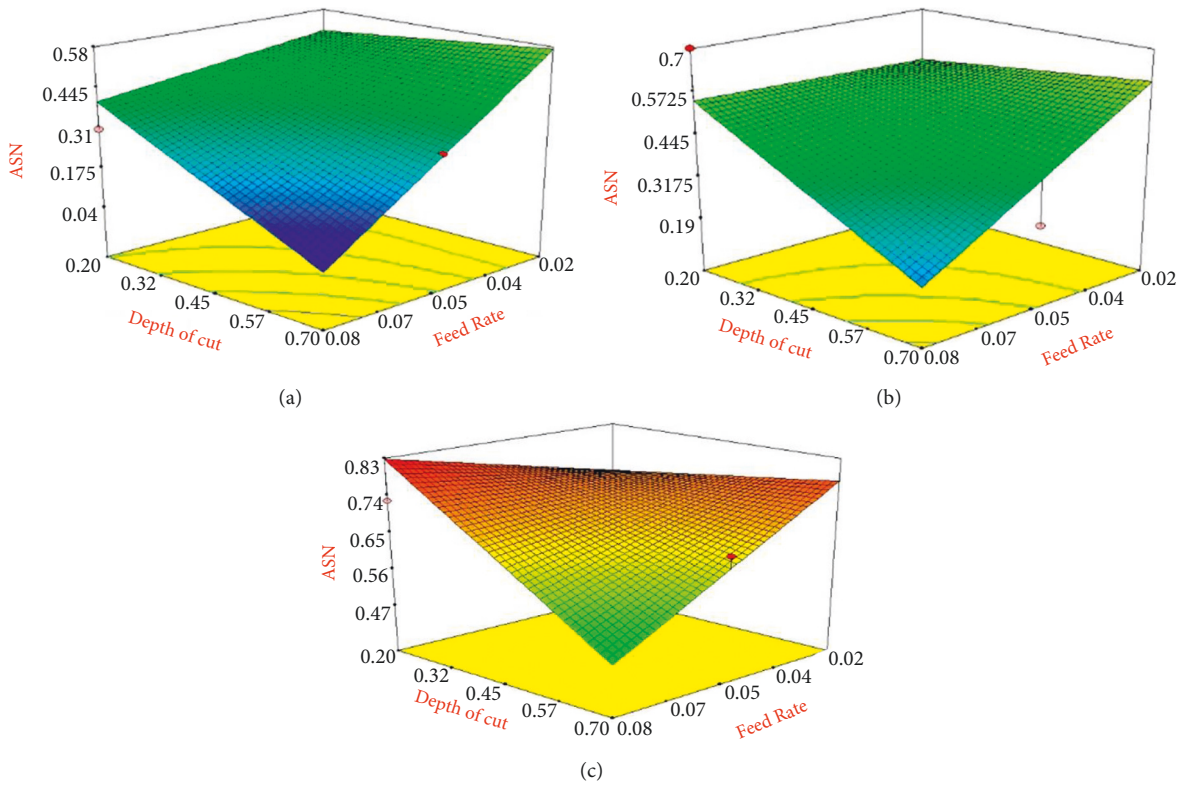

Figure 5: 3D response surface plots: (a) TiAlN, (b) ceramic, and (c) CBN.

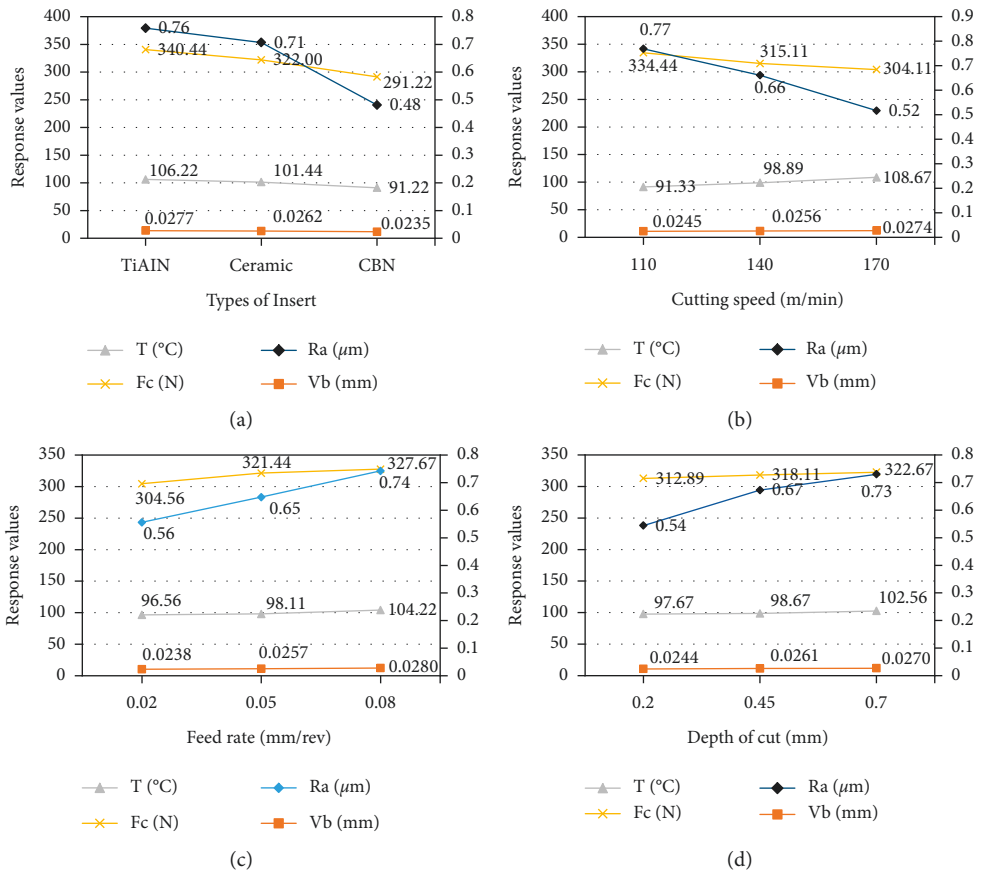

Figure 6: Effect of responses on (a) type of insert, (b) cutting speed, (c) feed rate, and (d) depth of cut.

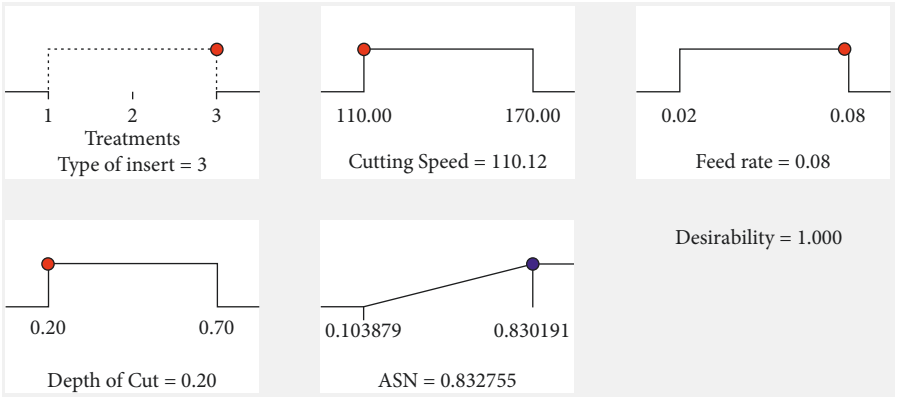

Figure 7: Ramp graph for desirability index.

Table 6: Optimal machining condition.

Factor	Name	Optimal level	Low level	High level
A	Type of insert	CBN	TiAlN	CBN
B	Vc	110.12	110	170
C	F	0.079	0.02	0.08
D	Depth of cut	0.20076	0.2	0.7
Response	Prediction	SE mean	95% CI low	95% CI high
ASN	0.8328	0.073	0.68	0.999

Table 7: Comparison of the response values of ASN setting and confirmation experiment.

Responses	ASN setting	Confirmation experiment	Improvement	Improvement in percentage
ASN	0.8301	0.8328	0.0027	0.3253
Surface roughness, SR (μm)	0.32	0.317	0.003	0.9375
Flank wear, FW (mm)	0.0213	0.0202	0.0011	5.1643
Temperature, T (°C)	98	76	22	22.4490
Cutting force, Fc (N)	289	259.2	29.8	10.3114

predicted optimal condition in improving the responses. The combo of turning variables with the highest ASN (0.8301) value, trial number 26 is used for comparison (Table 7). While turning with the ideal condition forecasted by the merged ASN-RSM method, there is a substantial improvement in the answers.

SEM images observed under the highest ASN setting (experiment no. 26) and confirmation experiment are displayed in Figure 8. The surface roughness profile, SEM images of machined surface, worn-out insert, and chips observed at experiment no. 26 (Figure 8(a)) were analyzed and compared with the confirmation experiment (Figure 8(b)). The machined profile reveals a better surface finish obtained during the confirmation experiment with the same setting used in trial 26. The surface waviness is restricted as well, and it is visualized in the P-profile graph. The SEM images of the machined surface show minimal and near-uniform machining marks in the surface obtained using the same setting. As explained in the previous sections, the cooling and lube nature of nMoS2 restrict the marks on the machined face. Reduced flank wear was seen in the confirmation experiment with the same setting and the improvement was around 0.0011. The received setting during the optimization has a positive effect on sustainable manufacturing. Similar to roughness and flank wear, the temperature and cutting force results are good with the same setting of experiment no. 26. Under the ASN setting and confirmation experiment, less jagged teeth were formed.

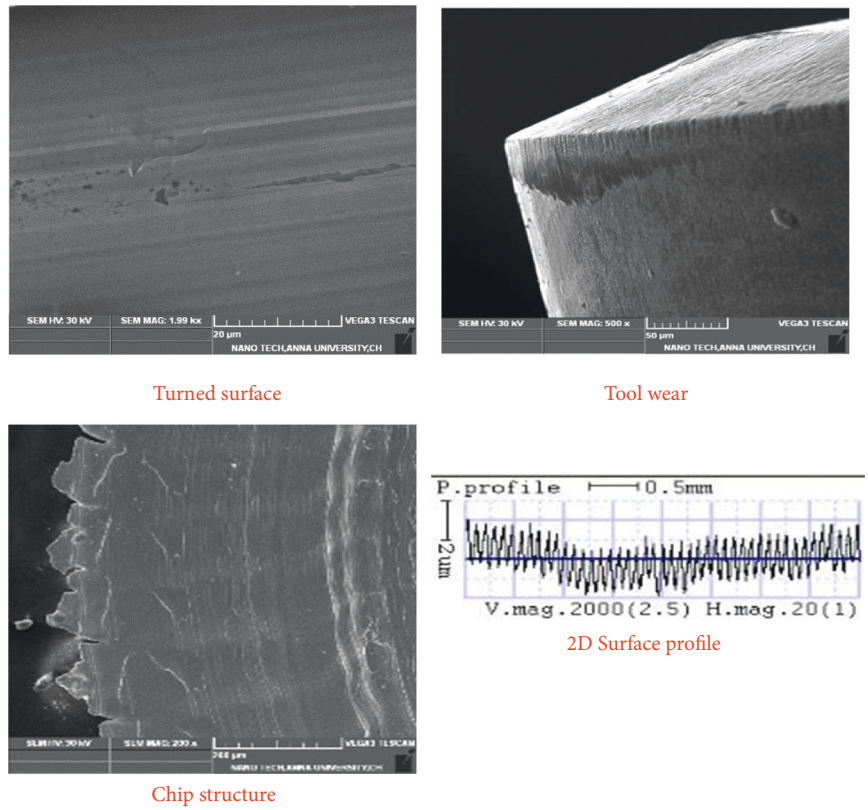

(a)

Figure 8: Continued.

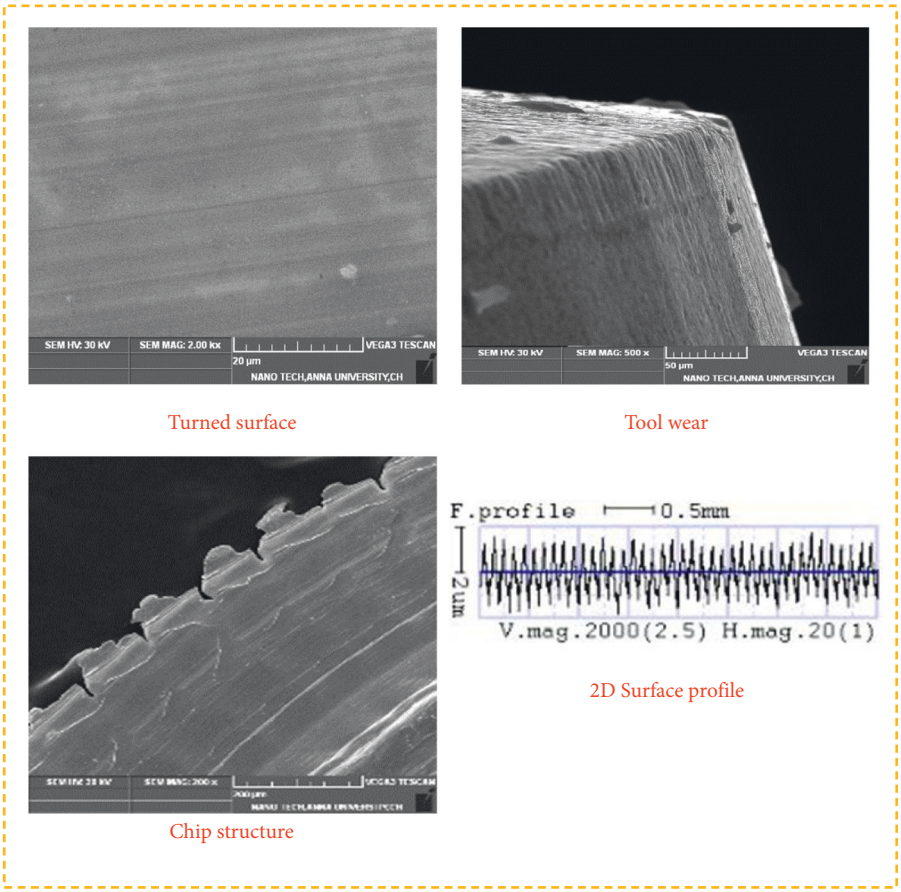

(b)

Figure 8: (a) Surface roughness profile and SEM images experiment no. 26 and (b) surface roughness profile and SEM images observed at the confirmation experiment.

5. Conclusions

The technique of MQL was observed to be effective in improving the machining characteristics of AISI O1 steel. An integrated approach of ASN-RSM was used to model the parameter for better responses and the desirability-based approach to arrive at the optimal parameter setting was validated through confirmation experiments. The following conclusions were drawn.

(i) The nMoS2 blended in biodegradable castor oil employed for lubrication had ensured a considerable reduction in temperature at the tool-work interface and hence could be a viable alternative to the traditional cutting fluids.

(ii) The optimal parameter setting under MQL environment is identified as follows: type of insert – CBN, Vc – 110.12 m/min, f – 0.079 mm/rev, and DOC – 0.20076 mm.

(iii) The statistical supremacy of both Taguchi's S/N ratio concept and RSM are combined to arrive at the optimal setting of parameters. The integration of the two techniques can be realized as the multiple variables are transformed into a single quality index (ASN), which acts as the representative of the various responses. The predicted polynomial model was also observed to be fit and precise.

(iv) The surface finish and tool wear observed at the optimal machining condition were significantly lower than that obtained using the initial setting of parameters. The work offers the necessary direction to handle AISI O1 steel in tool and dies industries under the MQL environment.

Data Availability

The data used to support the findings of this study are included in the article. Should further data or information be required, these are available from the corresponding author upon request.

Conflicts of Interest

The authors declare that they have no conflicts of interest.

References

[1] L. Bourithis, G. D. Papadimitriou, and J. Sideris, "Comparison of wear properties of tool steels AISI D2 and O1 with the same hardness," *Tribology International*, vol. 39, no. 6, pp. 479–489, 2006.

[2] V. García Navas, I. Ferreres, J. A. Marañón, C. Garcia-Rosales, and J. Gil Sevillano, "Electro-discharge machining (EDM) versus hard turning and grinding-Comparison of residual stresses and surface integrity generated in AISI O1 tool steel," *Journal of Materials Processing Technology*, vol. 195, pp. 186–194, 2008.

[3] C. Ezilarasan, V. S. Senthil kumar, and A. Velayudham, "An experimental analysis and measurement of process performances in machining of nimonic C-263 super alloy," *Measurement*, vol. 46, no. 1, pp. 185–199, 2013.

[4] S. Khani, M. Farahnakian, and M. R. Razfar, "Experimental study on hybrid cryogenic and plasma-enhanced turning of 17-4PH stainless steel," *Materials and Manufacturing Processes*, vol. 30, no. 7, pp. 868–874, 2015.

[5] A. Thakur and S. Gangopadhyay, "State-of-the-art in surface integrity in machining of nickel-based super alloys," *International Journal of Machine Tools and Manufacture*, vol. 100, pp. 25–54, 2016.

[6] S. Debnath, M. M. Reddy, and Q. S. Yi, "Environmental friendly cutting fluids and cooling techniques in machining: a review," *Journal of Cleaner Production*, vol. 83, pp. 33–47, 2014.

[7] Ç. Yildirim, T. Kivak, F. Erzincanli, İ. Uygur, and M. Sarikaya, "Optimization of MQL parameters using the Taguchi method in milling of nickel based waspaloy," *Gazi Univ. J. Sci.*vol. 30, pp. 173–186, 2017.

[8] E. Kuram, B. Ozcelik, and P. E. Demirbas, "Environmentally friendly machining: vegetable based cutting fluids," *Presented at the January*, vol. 1, 2013.

[9] M. H. S. Elmunafi, D. Kurniawan, and M. Y. Noordin, "Use of Castor oil as cutting fluid in machining of hardened stainless steel with minimum quantity of lubricant," *Procedia CIRP*, vol. 26, pp. 408–411, 2015.

[10] R. W. Maruda, G. M. Krolczyk, E. Feldshtein, P. Nieslony, B. Tyliszczak, and F. Pusavec, "Tool wear characterizations in finish turning of AISI 1045 carbon steel for MQCL conditions," *Wear*, vol. 372, pp. 54–67, 2017.

[11] D. A. Stephenson, S. J. Skerlos, A. S. King, and S. D. Supekar, "Rough turning Inconel 750 with supercritical CO2-based minimum quantity lubrication," *Journal of Materials Processing Technology*, vol. 214, no. 3, pp. 673–680, 2014.

[12] R. Heinemann, S. Hinduja, G. Barrow, and G. Petuelli, "Effect of MQL on the tool life of small twist drills in deep-hole drilling," *International Journal of Machine Tools and Manufacture*, vol. 46, no. 1, pp. 1–6, 2006.

[13] M. K. Gupta, P. K. Sood, and V. S. Sharma, "Machining parameters optimization of titanium alloy using response surface methodology and particle swarm optimization under minimum-quantity lubrication environment," *Materials and Manufacturing Processes*, vol. 31, no. 13, pp. 1671–1682, 2016.

[14] R. Saidur, K. Y. Leong, and H. A. Mohammed, "A review on applications and challenges of nanofluids," *Renewable and Sustainable Energy Reviews*, vol. 15, no. 3, pp. 1646–1668, 2011.

[15] C. Mao, Y. Huang, X. Zhou, H. Gan, J. Zhang, and Z. Zhou, "The tribological properties of nanofluid used in minimum quantity lubrication grinding," *International Journal of Advanced Manufacturing Technology*, vol. 71, no. 5-8, pp. 1221–1228, 2014.

[16] M. Zalaznik, M. Kalin, S. Novak, and G. Jakša, "Effect of the type, size and concentration of solid lubricants on the tribological properties of the polymer PEEK," *Wear*, vol. 364-365, pp. 31–39, 2016.

[17] A. K. Sharma, A. K. Tiwari, and A. R. Dixit, "Progress of nanofluid application in machining: a review," *Materials and Manufacturing Processes*, vol. 30, no. 7, pp. 813–828, 2015.

[18] Y. Zhang, C. Li, D. Jia, D. Zhang, and X. Zhang, "Experimental evaluation of MoS2 nanoparticles in jet MQL grinding with different types of vegetable oil as base oil," *Journal of Cleaner Production*, vol. 87, pp. 930–940, 2015.

[19] R. K. Singh, A. K. Sharma, A. R. Dixit, A. K. Tiwari, A. Pramanik, and A. Mandal, "Performance evaluation of alumina-graphene hybrid nano-cutting fluid in hard turning," *Journal of Cleaner Production*, vol. 162, pp. 830–845, 2017.

[20] R. Padmini, P. Vamsi Krishna, and G. Krishna Mohana Rao, "Effectiveness of vegetable oil based nanofluids as potential cutting fluids in turning AISI 1040 steel," *Tribology International*, vol. 94, pp. 490–501, 2016.

[21] P. Sivaiah, "Experimental investigation and modelling of MQL assisted turning process during machining of 15-5 PH stainless steel using response surface methodology," *SN Applied Sciences*, vol. 1, 2019.

[22] E. Bair, T. Hastie, D. Paul, and R. Tibshirani, "Prediction by supervised principal components," *Journal of the American Statistical Association*, vol. 101, no. 473, pp. 119–137, 2006.

[23] K. Ganesan, M. Naresh Babu, M. Santhanakumar, and N. Muthukrishnan, "Experimental investigation of copper nanofluid based minimum quantity lubrication in turning of H 11 steel," *Journal of the Brazilian Society of Mechanical Sciences and Engineering*, vol. 40, no. 3, p. 160, 2018.

[24] V. G. Navas, I. Ferreres, J. A. Maranon, C. G. Rosales, and J. G. Sevillano, "White layers generated in AISI O1 tool steel by hard turning or by EDM," *International Journal of Machining and Machinability of Materials*, vol. 4, no. 4, pp. 287–301, 2008.

[25] H. A. Kishawy, M. Dumitrescu, E.-G. Ng, and M. A. Elbestawi, "Effect of coolant strategy on tool performance, chip morphology and surface quality during high-speed machining of A356 aluminum alloy," *International Journal of Machine Tools and Manufacture*, vol. 45, no. 2, pp. 219–227, 2005.